

Received July 25, 2019; reviewed; accepted September 26, 2019

## Selective catalytic reduction of NO<sub>x</sub> with ammonia (NH<sub>3</sub>-SCR) over transition metal-based catalysts - influence of the catalysts support

Agnieszka Szymaszek, Bogdan Samojedon, Monika Motak

AGH University of Science and Technology, Faculty of Energy and Fuels, Al. Mickiewicza 30, 30-059 Kraków, Poland

Corresponding author: agnszym@agh.edu.pl (Agnieszka Szymaszek)

**Abstract:** Natural layered clays (bentonite and vermiculite) and natural zeolite (clinoptilolite) were tested and compared as the supports of the catalysts for selective catalytic reduction with ammonia (NH<sub>3</sub>-SCR). The raw materials were modified in order to improve their catalytic properties. Layered clays were treated with HNO<sub>3</sub> and intercalated with Al<sub>2</sub>O<sub>3</sub> pillars to enhance their acidity, porosity and specific surface area. Clinoptilolite was ion-exchanged with NH<sub>4</sub>NO<sub>3</sub> in order to increase the content of Brønsted acid sites, indispensable for NH<sub>3</sub> adsorption during the reaction. Subsequently, iron as an active phase was deposited on the modified supports by various methods, including incipient wetness impregnation, ion-exchange and co-precipitation. The efficiency of these methods was compared as NO<sub>x</sub> conversion obtained for each material. XRD analysis indicated that the initial modifications affected the structure of the raw aluminosilicates. FT-IR measurement confirmed the presence of characteristic Si-O and Al-O bonds and H<sub>2</sub>O molecules that occur naturally in the materials. UV-Vis spectroscopy results indicated that different types of Fe species were deposited on the catalysts surface and their form strongly depends on the type of the support. NH<sub>3</sub>-SCR catalytic tests showed that all of the analyzed materials exhibit satisfactory level of NO conversion and negligible concentration of by-product (N<sub>2</sub>O) in the exhaust gas. The highest catalytic activity (ca. 50% at 170°C and over 95% above 250°C) was obtained for Fe-Bent. The lowest concentration of N<sub>2</sub>O in the flue gas (less than 5 ppm in the whole temperature range) was observed for Fe-Clin.

**Keywords:** NH<sub>3</sub>-SCR, NO<sub>x</sub>, clinoptilolite, layered clays, iron

### 1. Introduction

The emission of hazardous pollutants is a serious environmental problem nowadays. One of the most dangerous substances produced by industry and transport are nitrogen oxides (NO<sub>x</sub>). For that reason, the latest EU legislations concerning the emission of NO<sub>x</sub> are becoming more and more restrictive (Motak, 2008; Guan et al., 2014; Wierzbicki et al., 2015). Techniques applied to reduce the generation of nitrogen oxides are divided into primary and secondary methods. The first group involves optimization of the fuel combustion process, in order to minimize the amount of NO<sub>x</sub> produced in the combustion zone. The second one is based on the treatment of NO<sub>x</sub> which are already present in the exhaust gas (Srivastava et al., 2005). The secondary measures are distinguished into catalytic and non-catalytic. The most widespread non-catalytic method is adsorption, especially onto activated carbons (Zhang et al., 2008; Barbooti et al., 2011, Woźniak et al., 2018). However, the main drawbacks of this solution are high cost of the most effective adsorbents and their expensive regeneration. Moreover, there is a high risk of the generation of secondary pollution when adsorption is applied. The control of NO<sub>x</sub> emission using catalytic measures can be based on selective or non-selective reduction by the reducing agent (NSCR and SCR, respectively) (Yang et al., 2014). Both processes involve the reaction between nitrogen oxide and ammonia or urea injected to the stream of flue gas. The main products of the reaction are molecular nitrogen and water vapour (Engler, 1991). However, application of non-selective catalytic reduction usually results in the formation of hazardous nitrogen species, such as N<sub>2</sub>O, NO or NO<sub>2</sub>. What is more,

in this case, there is a high risk that the reaction of ammonia oxidation proceeds at much higher rate than the reaction between  $\text{NO}_x$  and  $\text{NH}_3$  (Madia et al., 2002). Therefore, the most preferable method applied for the removal of  $\text{NO}_x$  is selective catalytic reduction with ammonia ( $\text{NH}_3$ -SCR). The commercial catalyst of this process is  $\text{V}_2\text{O}_5$ - $\text{TiO}_2$  on a ceramic monolith, promoted with  $\text{WO}_3$  or  $\text{MoO}_3$  (Grzybek, 2007). However, due to some significant operating problems, the application of this material is limited. First of all, the catalyst is most active at 350–400°C. Therefore, it should be installed upstream of the electrostatic precipitator and flue gas desulfurization equipment ("high-dust" position). In such a case, the catalyst undergoes contamination by  $\text{SO}_2$ , alkaline metals and the particles of fly ash. The reasonable solution would be to place the system at the "tail end" position, downstream the electrostatic precipitator. However, large amount of energy is necessary to increase the temperature of flue gas, so that the catalyst operates efficiently. Besides, the utilization of the vanadium catalyst can lead to the secondary contamination of the soil by poisonous vanadium species (Rahkamaa-Tolonen et al., 2005; Motak et al., 2015; Wierzbicki et al., 2015). Some studies also indicated that above 500°C the commercial V-based catalyst releases both vanadium and tungsten to the environment (Liu et al., 2015).

In this context, many studies have been devoted to the development of novel  $\text{NH}_3$ -SCR catalysts. One of the most significant factors that contributes to satisfactory performance is the choice of an appropriate support of the catalyst. It should have well-developed pore system that facilitates the access of gas molecules to the active centres. Moreover, it is preferable that it provides catalytically active sites itself and exhibits high thermal stability and durability.

A great number of scientific publications relate to promising supports of  $\text{NH}_3$ -SCR catalysts, such as activated carbons (Samojeden and Grzybek, 2016; Saad et al., 2019), zeolites (Niu et al., 2016; Martin et al., 2017; Rutkowska et al., 2017; Wang et al., 2019), cenosphers (Samojeden et al., 2019a, Samojeden et al., 2019b), supported metal oxides (Andreoli et al., 2015; Kwon et al., 2016) or hydrotalcite-derived mixed metal oxides (Wierzbicki et al., 2015; Jabłońska and Palkovits, 2016). Alternative group are modified layered clays (Grzybek, 2007; Motak, 2008; Chmielarz et al., 2011; Shen et al., 2014). The materials can be negatively or positively charged and are called cationic or anionic clays, respectively. The representative of naturally occurred cationic clays are bentonites, which consist predominantly of montmorillonite. Montmorillonites are built of one octahedral Al-based sheet situated between two tetrahedral Si-O sheets. Partial substitution of  $\text{Al}^{3+}$  by  $\text{Mg}^{2+}$  in the octahedral layer generates the excessive negative charge, which is neutralized by cations present in the interlayer space (Grzybek, 2007). Another example of common natural layered aluminosilicate is vermiculite (Chmielarz et al., 2009; Huff, 2016; Ziemiański, 2015). The material has a layered structure, but in contrast to bentonite, contains some significant amount of iron ions built up in the octahedral sheets (Stawiński et al., 2017). The large catalytic potential of layered materials results in many possibilities of their modification. The catalytic activity and selectivity can be easily increased by optimizing acidity and textural properties of the clays (Motak, 2008; Yuan et al., 2018). Moreover, the materials are abundant in the environment, therefore they can be easily acquired. Chmielarz et al. (Chmielarz et al., 2003) analyzed the influence of the preparation procedure of the modified montmorillonite on its catalytic performance in  $\text{NH}_3$ -SCR. The support was initially treated with the intercalating solution containing Al- or Ti-oligocations. The treatment led to the introduction of the pillars in the interlayer space via ion-exchange with the charge-balancing cations.  $S_{\text{BET}}$  analysis of the obtained supports showed that intercalation increased the specific surface area and micropore volume. The catalytic tests carried out over as prepared supports containing copper showed that above 250°C, the catalysts exhibited 90% conversion of NO and 95% selectivity towards  $\text{N}_2$ . Additionally, the presence of water vapour in the stream of the flue gas caused only negligible drop of NO conversion and the effect was fully reversible.

An alternative attempt to the modification of aluminosilicates was acid activation of vermiculites. According to the scientific literature, the treatment of the raw vermiculite with an oxidizing acid leads to the increase of surface acidity. Moreover, it results in the enlargement of the specific surface area and the volume of micropores. Another important result of acid activation is leaching of the octahedrally-coordinated  $\text{Fe}^{3+}$  cations present in the tetrahedral sheets of the material. Therefore, the external surface is enriched in new active sites, more accessible for  $\text{NH}_3$ -SCR (Chmielarz et al., 2008). The preparation procedure of acid treated vermiculites was described by Chmielarz et al. and Santos et al. (Chmielarz et al., 2012; Santos et al., 2015). The studies on the influence of the type and concentration of the leaching

acid indicated that the most preferable structural properties were obtained for materials treated with 0.8 mol·dm<sup>-3</sup> nitric acid. Moreover, it was proved that the duration of acid treatment determines the pore volume. The results of XRD studies suggested that the interlayer K<sup>+</sup> and Mg<sup>2+</sup> cations are replaced with H<sup>+</sup> and the interlayer distance is reduced during acid activation. It is expected, that the effect can be minimized when acid treatment is followed by pillaring. NH<sub>3</sub>-SCR catalytic tests carried out by Chmielarz et al. (Chmielarz et al., 2012) over acid-leached vermiculites indicated strong potential of these materials in NO reduction. However, the introduction of an active phase is indispensable to increase the conversion of nitrogen oxides in the whole temperature range.

Another group of aluminosilicates that can be efficiently used as NH<sub>3</sub>-SCR catalysts precursors are zeolites (Ma et al., 2013; Paolucci et al., 2016; Dakdareh et al., 2018). It is especially due to their surface acidity, outstanding hydrothermal stability and durability. These microporous crystalline materials are composed of SiO<sub>4</sub>- and AlO<sub>4</sub>-tetrahedra and can be formed naturally or prepared synthetically (Weckhuysen and Yu, 2015). Wang et al. (Wang et al., 2015) studied the catalytic performance of Cu-SAPO-34 in NH<sub>3</sub>-SCR and the impact of Brønsted acidity on the catalytic properties. The analysis included K- and H- forms of zeolites with copper as an active phase. The authors observed a strong correlation between the Brønsted acidity and catalytic activity. It was proved that direct adsorption of NH<sub>3</sub> on the metal active sites is much less favourable thermodynamically in comparison to the adsorption on zeolite surface. Thus, the molecule firstly interacts with the Brønsted acidic site and migrates to the Cu site, to form N<sub>2</sub> in the reaction with NO<sub>x</sub>. On the other hand, when the content of K<sup>+</sup> in the zeolite was increased, the catalytic performance deteriorated, especially in the high temperature range. The difference in the catalytic activity of the samples was correlated mainly with the decrease of the number of Brønsted acidic sites. It was concluded that appropriate pre-treatment of the zeolite and its enrichment in Brønsted acidic sites is a crucial factor for effective NH<sub>3</sub>-SCR reaction.

Another important issue for the high catalytic activity is the active phase of the catalyst. Among many metals tested in NH<sub>3</sub>-SCR, the most satisfactory results were obtained for iron (Gao et al., 2016; Samojeden and Grzybek, 2016) and copper (Gao et al., 2015; Niu et al., 2016). However, copper has a tendency to oxidize ammonia above 350°C and as a result the conversion of NO decreases (Kowalczyk et al., 2018). Therefore, iron is more preferable, mainly due to the stability at high temperature and weakly-oxidizing properties. Moreover, iron is non-poisonous metal with high tolerance to the presence of SO<sub>x</sub> in the flue gas (Deng et al., 2016; Ryu et al., 2019). Additionally, the price of iron is relatively low in comparison to copper. Considering effective NH<sub>3</sub>-SCR catalysts, the issue of their utilization cannot be omitted. The most efficient method that can be used for the recovery of the solid-state catalysts from metal ions is flotation. High efficiency of this technique in the recovery of iron, copper, lead, zinc or vanadium was reported in detail in the scientific literature (Wan-Zhong et al., 2010; Deliyanni et al., 2017; Feng et al., 2019; Zhao et al., 2019).

Significant number of publications confirmed the excellent catalytic activity of aluminosilicate-supported catalysts modified with transition metals. However, a direct comparison of the properties of the naturally derived supports (layered clays and natural zeolites) have not been presented yet. Therefore, the paper presents the full analysis of the influence of the naturally-derived support on the catalytic performance in NH<sub>3</sub>-SCR.

## 2. Materials and methods

### 2.1. Catalysts preparation

The aluminosilicate-based catalysts were prepared by three different methods described in the subsections 2.1.-2.3. Introduction of Fe as the active phase was diversified for each material in order to obtain different forms of the active phase (from small crystallites to agglomerates and bulk species). The iron content was set down to reach approximately 5 wt.%. The list of prepared samples and their designation is presented in Table 1.

#### 2.1.1. Bentonite-supported catalyst

In order to obtain the bentonite-supported catalyst, the following steps were taken: in order to isolate the montmorillonite phase, raw bentonite (Fisher Scientific UK) was ion-exchanged with 3 mol·dm<sup>-3</sup>

Table 1. The list of the prepared samples

Designation of the sample	Support	Modification procedure
Mod-Bent	Bentonite (Bent)	acid treatment, pillaring with Al-oligocations
Fe-Bent		acid treatment, pillaring with Al-oligocations, Fe introduction by wet incipient impregnation
H-Clin	Clinoptilolite (Clin)	NH <sub>4</sub> NO <sub>3</sub> ion-exchange
Fe-Clin		NH <sub>4</sub> NO <sub>3</sub> ion-exchange, Fe introduction by co-precipitation
Mod-Verm	Vermiculite (Verm)	acid treatment, pillaring with Al-oligocations
Fe-Verm		acid treatment, pillaring with Al-oligocations, Fe introduction by ion-exchange

solution of NaCl at 95°C for 5 h. The action was repeated five times. Then, Na-bentonite was acid leached using 0.8 mol·dm<sup>-3</sup> solution of HNO<sub>3</sub>: 20 g of the sample was introduced into 200 cm<sup>3</sup> of the acid and left to react at 100°C for 4 h. Afterwards, the material was dried at 120°C for 24 h and calcined at 500°C for 5 h. The stabilization of the structure was provided by the treatment of the sample with 0.12 mol·dm<sup>-3</sup> of oxalic acid for 1 h, drying at 120°C for 24 h and calcination at 500°C for 5 h. In order to obtain Al-pillared bentonite, the material was ion-exchanged with the aluminum hydroxy-oligometric solution prepared using the route described by Chmielarz et al. (Chmielarz et al., 2003). The pillaring solution was added dropwise to the 3 wt.% suspension of the Na-bentonite in distilled water until the ratio of Al/Na-bentonite reached 12 mmol/g. The obtained suspension was left to react for 24 h at the room temperature under constant stirring. Afterwards, the material was dried at 120°C for 24 h and calcined at 500°C for 12 h. The Fe-containing active phase was introduced into the modified bentonite by wet incipient impregnation using aqueous solution of iron nitrate. The material was dried at 120°C for 24 h and calcined at 350°C for 4 h. The sample was labelled as Fe-Bent.

### 2.1.2. Vermiculite-supported catalyst

Vermiculite-supported catalysts were prepared via acid treatment and pillaring, similarly as bentonite-based materials described in the subsection 2.1.1. In this case, ion-exchange with the 3 mol·dm<sup>-3</sup> solution of NaCl was carried out five times before pillaring with Al-oligocations. The Fe-containing active phase was introduced into the structure of modified vermiculite by ion-exchange. 10 g of the modified support was added to 1000 cm<sup>3</sup> of iron nitrate solution. The suspension was vigorously stirred for 24 h. The obtained product was filtered, washed with distilled water and dried at 120°C for 24 h. Afterwards, the sample was calcined at 350°C for 4 h and labelled as Fe-Verm.

### 2.1.3. Clinoptilolite-supported catalyst

The natural zeolite (clinoptilolite) was initially transformed into H-form using 1 mol·dm<sup>-3</sup> aqueous solution of NH<sub>4</sub>NO<sub>3</sub>. The process was carried out at 90°C for 5 h and repeated five times. The Fe-containing active phase was introduced into the structure of H-zeolite using co-precipitation procedure, described by Śliwińska-Dąbrowska et al. (Śliwińska-Dąbrowska et al., 2011): 10 g of the H-zeolite was dispersed in a 0.05 mol·dm<sup>-3</sup> solution of FeSO<sub>4</sub> and vigorously stirred. The suspension was left to interact at 50°C for 4 h, maintaining the pH of 3.0. Afterwards, pH of the mixture was increased to 9.0 by the slow addition of 25% aqueous solution of NH<sub>3</sub>. The alkaline suspension was stirred for 1 h and then the product was filtered and washed several times with distilled water. Modified zeolite with precipitated iron was dried at 120°C for 24 h and calcined at 450°C for 2 h. The sample was labelled as Fe-Clin.

## 2.2. Catalysts characterization

The mineralogical composition and structural properties of the samples were determined by the XRD analysis. The X-ray diffraction patterns were obtained using Empyrean (Panalytical) diffractometer. The instrument was equipped with copper-based anode (Cu-K<sub>α</sub> LFF HR, λ = 0.154059 nm). The diffractograms were collected in the 2θ range of 2.0-80.0° (2θ step scans of 0.02° and a counting time of 1 s per step). The UV-Vis spectroscopy was applied to determine the coordination

and aggregation of iron species introduced onto the supports. The spectra were recorded using Lambda 35 UV-Vis Spectrophotometer in the range of 200-900 nm with a resolution of 1 nm. Fourier-transform-infrared spectroscopy (FT-IR) was performed to examine the characteristic chemical groups present in the structure of the analyzed materials. The spectra were recorded on a Thermo Nicolet 380 FT-IR spectrometer in the region of 4000-400  $\text{cm}^{-1}$  with a resolution of 4  $\text{cm}^{-1}$ . Before each measurement, the analyzed sample was mixed with KBr at the ratio of 1:100 and pressed into a disk.

### 2.3. Catalytic tests

The catalytic experiments were performed in a fixed-bed flow microreactor system under atmospheric pressure. 0.2 g of the sample was pre-treated *in situ* in the reactor in a flow of helium at 400°C for 1 h. The reaction mixture contained 800 ppm of NO, 800 ppm of  $\text{NH}_3$ , 3.5 vol. % of  $\text{O}_2$  and balance He. The total flow was 100  $\text{cm}^3 \cdot \text{min}^{-1}$ . The concentration of unreacted NO and  $\text{N}_2\text{O}$  (the by-product of the reaction) were analysed downstream of the reactor by FT-IR detector (ABB 2000 AO series). The reactor was heated to appropriate temperature (150, 200, 250, 300, 350 or 400°C, 10°C·min<sup>-1</sup>), which was controlled by an electronic thermocouple (Lumel RE19) placed in the catalyst bed. The temperature ramps were set up for 60 min. NO conversion was calculated according to the equation (1):

$$NO_{conversion} = \frac{NO_{inlet} - NO_{outlet}}{NO_{inlet}} \cdot 100\% . \quad (1)$$

## 3. Results

### 3.1. Catalysts characterization

#### 3.1.1. XRD patterns

The X-ray diffraction (XRD) patterns of the analyzed samples are shown in Figs. 1-3. The results obtained for natural clinoptilolite (Clin), H-form of clinoptilolite (H-Clin) and clinoptilolite with precipitated iron (Fe-Clin) are presented in Fig. 1. The lines characteristic for the crystalline zeolite structure are located at  $2\theta$  values of 10.0, 11.4, 17.3, 19.1, 22.5, 26.5, 28.1, 30.1 and 31.8°. The observed reflections are in agreement with the literature data (Nezamzadeh-Ejehieh and Amiri, 2013). Thus, it can be concluded that the main component of the sample is zeolitic phase. Comparing XRD patterns recorded for the parent clinoptilolite with those of H-Clin and Fe-Clin, it can be noticed that some significant differences occurred. After ion-exchange with  $\text{NH}_4\text{NO}_3$ , the intensity of the selected structural reflections (11.4, 30.1°) slightly decreased. The introduction of Fe species via co-precipitation and further calcination resulted in broadening of the most reflections of zeolite (11.4, 19.1, 22.5, 26.5, 28.1, 30.1, 31.8°). Active phase in the form of  $\text{Fe}_x\text{O}_y$  species can be observed at  $2\theta$  values of 26.6, 28.1, 32.0, 35.7, 40.6 and 63.8°. (Crystallography Open Database; Hirano, 1986).

XRD patterns of non-modified bentonite (Bent), acid treated and pillared bentonite (Mod-Bent) and bentonite impregnated with iron (Fe-Bent) are presented in Fig. 2. The patterns indicate that montmorillonite is the major component of the natural bentonite. The characteristic position of (001) reflection connected with the layered structure of the material was shifted to the lower values of  $2\theta$  after acid treatment and intercalation. Therefore,  $\text{Al}_2\text{O}_3$  pillars were successfully introduced into the interlayer space of the material. Other structural reflections of montmorillonite remained unchanged. Additionally, reflections observed at  $2\theta$  of 26.4 and 36.8° suggest the presence of quartz and other impurities in the sample. The calcination procedure carried out several times did not influence significantly the structure of the clay. Therefore, bentonite is expected to be stable to 500°C. The deposition of the active phase did not result in any structural changes and iron was successfully introduced in a form of  $\text{Fe}_x\text{O}_y$  species. The obtained results are in full agreement with Hirano (Hirano, 1986).

The XRD diffraction patterns obtained for parent vermiculite (Verm), acid treated and Al-pillared vermiculite (Mod-Verm) as well as vermiculite after the introduction of Fe via ion-exchange procedure (Fe-Verm) are presented in Fig. 3. The parent material exhibited lines at about 7.6° and 8.9°, confirming the presence of partially dehydrated interlayer  $\text{Mg}^{2+}$  and interlayer  $\text{K}^+$  cations, respectively (Chmielarz et al., 2008). The reflection at about 25° corresponds to quartz impurities in the sample. It can be

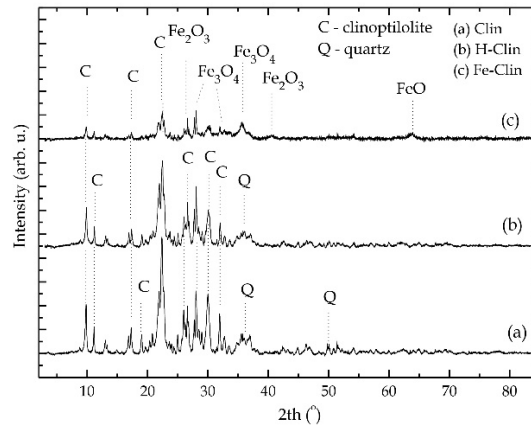


Fig. 1. X-ray diffraction patterns of clinoptililite and its modified forms: natural clinoptililite (a), H-clinoptililite (b), Fe-clinoptililite (c)

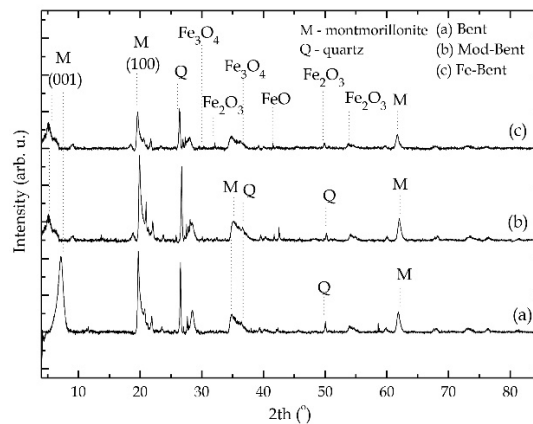


Fig. 2. X-ray diffraction patterns of parent bentonite and its modified forms: natural bentonite (a), acid treated and Al<sub>2</sub>O<sub>3</sub>-pillared bentonite (b), Fe-bentonite (c)

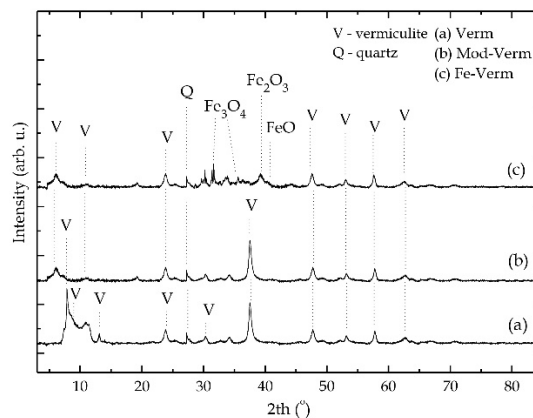


Fig. 3. X-ray diffraction patterns of vermiculite and its modified forms: natural vermiculite (a), acid treated and Al<sub>2</sub>O<sub>3</sub>-pillared vermiculite (b), Fe-vermiculite (c)

observed that acid activation and intercalation with Al<sub>2</sub>O<sub>3</sub> considerably influenced the final structure of vermiculite. The reflections at 7.6° and 8.9° disappeared completely, while a new one appeared at 6.0°. The effect may have arisen from the ion-exchange of interlayer cations with hydronium ions during the acid treatment. Additionally, another reflection can be assigned to Al<sub>2</sub>O<sub>3</sub> pillars successfully introduced into the interlayer space of vermiculite (Chmielarz et al., 2009). Other diffraction lines of vermiculite remained unchanged after the modification. The reflection at about 26.7° is assigned to the presence of

amorphous silica (Wu et al., 2009). After introduction of the active phase, new lines related to  $\text{Fe}_x\text{O}_y$  species appeared. The deposition of Fe did not result in any further structural changes of the modified vermiculite.

### 3.1.2. FT-IR characterization

The FT-IR spectra of modified aluminosilicates with deposited iron are presented in Fig. 4. The IR wavelength ranges of interest are O-H stretching vibrations ( $3800\text{-}3400\text{ cm}^{-1}$ ), Si-O stretching vibrations, Al-Me-OH bending vibrations, OH bending vibrations from  $\text{H}_2\text{O}$  ( $1700\text{-}700\text{ cm}^{-1}$ ) and pseudo lattice vibrations range ( $700\text{-}450\text{ cm}^{-1}$ ).

For Fe-Clin, the broad bands at  $3745\text{ cm}^{-1}$  and  $3720\text{ cm}^{-1}$  are assigned to Si-OH groups on external surfaces and in lattice defects. The band in the range of  $3680\text{-}3670\text{ cm}^{-1}$  can be ascribed to the weakly acidic, isolated  $\text{Fe}^{3+}\text{-OH}$  hydroxyls species, while the one at  $3525\text{ cm}^{-1}$  confirms the presence of Si(O-H)Al groups in the sample. Typically for Fe-exchanged zeolites, the intensity of the band at  $3610\text{ cm}^{-1}$  associated with Si(OH)Al groups is very low (Doula, 2007). Additionally, the intense peak at  $1631\text{ cm}^{-1}$  confirms the presence of bending vibration of water molecules in the zeolite. The broad band at  $1048\text{ cm}^{-1}$  is ascribed to the asymmetric O-Me-O stretching vibration ( $\text{Me} = \text{Al}^{3+}$  or  $\text{Si}^{4+}$ ), while the ones in the pseudo lattice vibrations range at  $649\text{ cm}^{-1}$  and  $470\text{ cm}^{-1}$  arise from the symmetric stretching vibrations of the tetrahedral groups of  $\text{AlO}_4$  and  $\text{SiO}_4$ , respectively. The bands present at  $602\text{ cm}^{-1}$  and  $1202\text{ cm}^{-1}$  are related to the O-Al-O or O-Si-O bending and Al-O or Si-O asymmetric stretching vibrations of the free tetrahedral groups. The peak of symmetric O-Al-O or O-Si-O stretching vibrations can be observed at  $734\text{ cm}^{-1}$ , whereas the band at  $524\text{ cm}^{-1}$  confirms so called "pore opening" vibration of the zeolite (Doula, 2003).

For the bentonite-based catalyst (Fe-Bent), three main absorption bands in -OH stretching region can be distinguished. The sharp peaks at  $3697\text{ cm}^{-1}$  and  $3440\text{ cm}^{-1}$  are related to the presence of water molecules in the interlayer space, whereas the one at  $3655\text{ cm}^{-1}$  indicates the presence of Brønsted acid sites in the clay. Similarly for Fe-Clin, the band at  $1634\text{ cm}^{-1}$  indicating the presence of bending vibrations of interlayer water can be observed. Three intense bands registered at  $875\text{ cm}^{-1}$ ,  $836\text{ cm}^{-1}$  and  $629\text{ cm}^{-1}$  are ascribed to hydroxyl bending vibration of  $\text{AlFeOH}$ ,  $\text{AlMgOH}$  and the presence of quartz, respectively. The broad band at  $1035\text{ cm}^{-1}$  and low-intensity peak at  $461\text{ cm}^{-1}$  are assigned to the Si-O stretching vibrations and symmetric stretching vibrations of the tetrahedral groups, respectively (Zhirong et al., 2011; Hayati-Ashtiani, 2012). The FT-IR spectra of Fe-Verm exhibited two absorption bands in the -OH vibration region:  $3716\text{ cm}^{-1}$  and  $3436\text{ cm}^{-1}$ . The first is assigned to the stretching vibrations of O-H in  $\text{Mg}_3\text{OH}$  or  $\text{Mg}_2\text{FeOH}$  groups in the vermiculite structure, while the second corresponds to the stretching vibration of the interlayer water. The additional sharp band at  $1636\text{ cm}^{-1}$  is related to the presence of bending vibration of  $\text{H}_2\text{O}$  molecules. The peaks at  $990\text{ cm}^{-1}$  and  $685\text{ cm}^{-1}$  arise from the presence of strong and weak Si-O or Al-O stretching vibrations, respectively. Bending vibrations of Al-O-Si and  $\text{AlMgOH}$  are confirmed by the bands at  $746\text{ cm}^{-1}$  and  $797\text{ cm}^{-1}$ , respectively. Finally, the peaks at  $1080\text{ cm}^{-1}$  and  $460\text{ cm}^{-1}$  arise from bending and stretching vibrations of  $\text{SiO}_4$  tetrahedra, respectively (Huo et al., 2012).

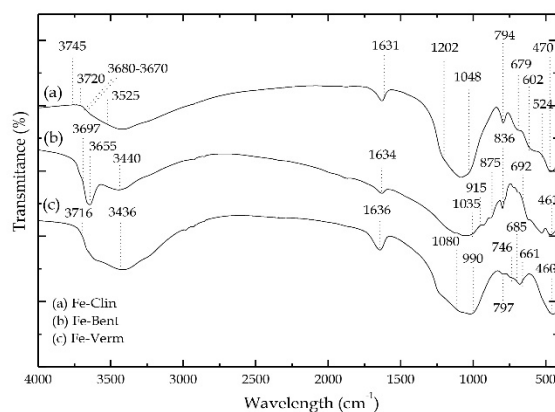


Fig. 4. FT-IR spectra of Fe-Clin (a), Fe-Bent (b), Fe-Verm (c) in a region of  $4000\text{ to }450\text{ cm}^{-1}$

### 3.1.3. UV-Vis spectroscopy studies

The UV-Vis spectroscopy allowed to determine various forms of iron species deposited on the modified supports. The observed bands are related to  $\text{Fe}^{3+} \leftarrow \text{O}$  charge transfer and their position is determined by coordination and aggregation of iron species. The spectra of the parent aluminosilicates and the modified materials with Fe are presented in Fig. 5. The initial modifications and deposition of the active phase significantly influenced the shape of the spectra as compared to the parent materials. Raw clinoptilolite (a) and raw bentonite (c) did not exhibit any bands characteristic for metal species. On the other hand, the band at about 260 nm, which was registered for raw vermiculite (e), suggests the presence of isolated  $\text{Fe}^{3+}$  cations in the octahedral coordination. The result is in good agreement with the theory concerning the occurrence of these cations in the original vermiculite structure (Rey-Perez-Caballero and Poncelet, 2000). The introduction of iron resulted in some significant changes in absorption spectra obtained for all of the analyzed samples. The band at 214 nm, observed for Fe-Clin and Fe-Bent, is assigned to well-dispersed  $\text{Fe}^{3+}$  isolated cations in the tetrahedral coordination. The peak at 260 nm detected for Fe-Bent suggests that a part of iron was built into the octahedral sheets. The bands at 460 nm, 625 nm and 685 nm, observed for all materials, are due to the presence of bulky and aggregated  $\text{Fe}_2\text{O}_3$  species deposited on the external surface. The most intense bands assigned to these forms are detected for Fe-Verm. It is predicted that these species may affect the selectivity to  $\text{N}_2$  in the  $\text{NH}_3$ -SCR. The peak at 340 nm detected for Fe-Verm indicates the presence of small oligonuclear  $\text{Fe}_x\text{O}_y$  clusters located in the interlayer space or at the surface of the material (Chmielarz et al., 2010).

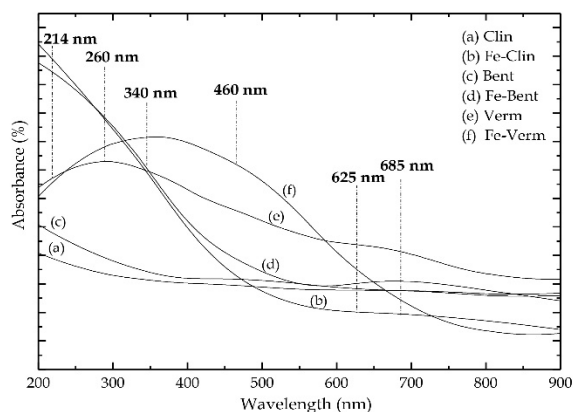


Fig. 5. UV-Vis spectra of Clin (a), Fe-Clin (b), Bent (c), Fe-Bent (d), Verm (e), Fe-Verm (f)

### 3.2. $\text{NH}_3$ -SCR performance

The results of catalytic studies are summarized in Fig. 6a. and 6b. All of the analyzed materials exhibited excellent activity, reaching at least ca. 85% of NO conversion at 250°C and ca. 100% at 300°C. The highest activity at the lowest temperature (150°C) was detected for Fe-Bent, while the results obtained for Fe-Verm and Fe-Clin were ca. twice lower and similar to each other. Above 350°C the catalytic activity of Fe-Verm is considerably lower than that of the other tested catalysts. The selectivity to  $\text{N}_2$  was satisfactory for all of the analyzed catalysts, as the amount of emitted  $\text{N}_2\text{O}$  did not exceed 30 ppm (the experimental error is ca. 30 ppm). The lowest concentration of the by-product was detected for Fe-Clin, while the highest was exhibited by Fe-Bent.

## 4. Discussion

It was observed that the initial modifications of the raw aluminosilicates influenced differently on the final structure of the supports. XRD analysis indicated that in case of natural zeolite, transformation into H-form and co-precipitation of iron changed the structural properties of the zeolitic lattice. Crystallinity of the sample was considerably lowered and some reflections characteristic for zeolite structure disappeared. It is predicted that the damages may be related to the high temperature of calcination. In contrast, in case of layered materials, most of the characteristic reflections remained un-

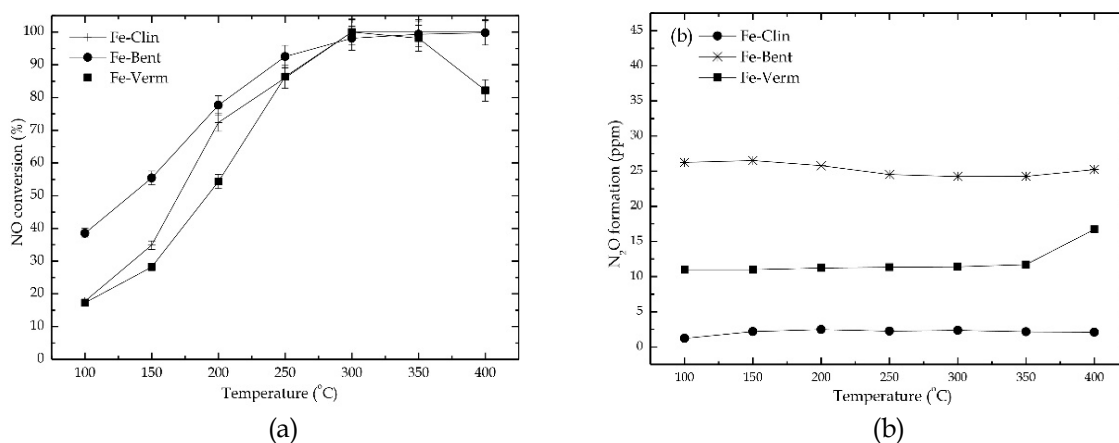


Fig. 6. NH<sub>3</sub>-SCR catalytic performance of the studied samples: NO conversion (a), N<sub>2</sub>O formation (b) (experimental conditions: [NO] = 800 ppm, [NH<sub>3</sub>] = 800 ppm, [O<sub>2</sub>] = 3.5 vol.%, balance He, total flow of the gas mixture: 100 cm<sup>3</sup>·min<sup>-1</sup>, mass of the catalyst: 200 mg)

changed upon calcination. Therefore, the materials are more preferable while SCR reaction is carried out in the high temperature range (above 400°C).

Both the structure of the supports and the form of active phase reflect the results of catalytic tests. The highest activity in NO conversion obtained for Fe-Bent is probably correlated with the presence of various bulky Fe species deposited on the catalyst surface and high thermal stability of the material. Additionally, the satisfactory catalytic performance was facilitated by the increased acidity and enlarged interlayer distance provided by acid activation and intercalation, respectively. The results are in full agreement with those obtained by Chmielarz et al. and Motak (Chmielarz et al., 2004; Motak, 2008). The lowest NO conversion among all of the tested catalysts was reached by Fe-Verm. The results obtained for that sample are comparable to the other materials only in a narrow temperature range of 300-350°C. The high conversion of Fe-Verm in this region may have originated from the presence of some amount of Fe in the octahedral sheets of the parent clay. Additionally, it is possible that the intercalation procedure was not as successive as in case of Fe-Bent. As a consequence, the diffusion of gas molecules to the active sites present in the interlayer space was limited. Similar results were obtained by Chmielarz et al. (Chmielarz et al., 2008). Intermediate amount of N<sub>2</sub>O in the flue gas detected for Fe-Verm can be related both to the lowest catalytic activity and co-existence of various Fe species deposited upon ion-exchange. The highest amount of N<sub>2</sub>O was emitted by Fe-Bent. The effect can be correlated with the considerable quantity of bulk Fe<sub>x</sub>O<sub>y</sub> species deposited in the interlayer space and on the tetrahedral sheets of bentonite, confirmed by XRD and UV-Vis. On the other hand, the lowest formation of the by-product was detected for Fe-Clin, mainly due to the presence of dispersed isolated Fe<sup>3+</sup> cations. Additionally, well-developed pore system of the zeolite might facilitate the access of the gas molecules to the active species on the support. Therefore, co-precipitation combined with the appropriate modification of zeolite resulted in the formation of highly effective SCR catalytic system.

The catalytic performance of the obtained catalysts was compared to the selected materials reported in the scientific literature. The results of the catalytic tests with the distinction for layered clays and zeolites are presented in Table 2. Additionally, the catalytic performance was compared to the commercial V-based catalyst.

As it is presented in Table 2, the catalytic performance of the prepared materials is similar or even better than that for the catalysts reported in the cited literature. The commercial V-based system reaches ca. 100% of NO conversion in the temperature range of 300-450°C, while the prepared aluminosilicate-supported catalysts exhibit only negligibly lower activity, but at 300-350°C. Additionally, the formation of N<sub>2</sub>O obtained for the prepared samples does not exceed 30 ppm. Thus, the selectivity is comparable to the one of V<sub>2</sub>O<sub>5</sub>-WO<sub>3</sub>/TiO<sub>2</sub>. Therefore, the materials may be used as effective and cheaper substitutes of the commercial one. The catalytic performance of Fe-Clin is much better than in case of the one reported by Gelves et al. (Gelves et al., 2019). It can be concluded that co-precipitation is more preferable method than ion-exchange, while Fe is deposited on the zeolite surface. Considering catalytic

performance of the layered clays, it was observed that NO conversion reached higher level at the lower temperature range than in case of the results reported by Chmielarz et al. (Chmielarz et al., 2009). The reason of such result may be determined by the efficiency of initial modifications or the procedure of active phase deposition.

Table 2. Research results on several kinds of aluminosilicate-based SCR catalysts

Type of the catalyst	Preparation procedure	Highest NO conversion (temperature range)	N <sub>2</sub> O formation or N <sub>2</sub> selectivity	Reference
V <sub>2</sub> O <sub>5</sub> -WO <sub>3</sub> /TiO <sub>2</sub>	impregnation (calc. 500°C)	100% (300-450°C)	15 ppm N <sub>2</sub> O	(Chen et al., 2011)
Fe-exchanged natural zeolite	ion-exchange (calc. 360°C)	85% (400-450°C)	170 ppm N <sub>2</sub> O	(Gelves et al., 2019)
<b>Fe-Clin</b>	<b>co-precipitation (calc. 450°C)</b>	<b>95% (300-350°C)</b>	<b>&lt; 5 ppm N<sub>2</sub>O</b>	-
Fe-doped montmorillonite	ion-exchange (calc. 450°C)	90% (450°C)	93% of N <sub>2</sub> selectivity	(Chmielarz et al. 2009)
<b>Fe-Bent</b>	<b>impregnation (calc. 350°C)</b>	<b>98% (300-350°C)</b>	<b>31 ppm N<sub>2</sub>O</b>	-
Fe-doped vermiculite	ion-exchange (calc. 450°C)	100% (400-450°C)	96% of N <sub>2</sub> selectivity	(Chmielarz et al. 2009)
<b>Fe-Verm</b>	<b>Ion-exchange (calc. 350°C)</b>	<b>96% (300-350°C)</b>	<b>25 ppm N<sub>2</sub>O</b>	-

## 5. Conclusions

Natural layered aluminosilicates (bentonite and vermiculite) and natural zeolite (clinoptilolite) were modified, doped with iron and tested as NH<sub>3</sub>-SCR catalysts. The initial modification of the layered materials included acid treatment and pillaring with Al<sub>2</sub>O<sub>3</sub>. The pretreatment of the natural zeolite resulted in lowered crystallinity. XRD and UV-Vis proved successful introduction of Fe-active phase for all of the materials. It was observed that the deposition of Fe influenced both the form of iron species and the final structure of the support.

The catalytic performance in NH<sub>3</sub>-SCR was satisfactory for all of the analyzed samples. The highest activity was obtained for Fe-Bent, where the NO conversion was ca. 50% at about 170°C (*T*<sub>50</sub>) and over 95% above 250°C. However, the concentration of N<sub>2</sub>O was the highest for this material. Therefore, the best results were obtained for Fe-Clin that exhibited ca. 100% NO conversion at 300°C and less than 5 ppm of N<sub>2</sub>O in the flue gas in the whole temperature range. Additionally, only vermiculite-supported material catalyzed the reaction of ammonia oxidation above 350°C.

The results obtained for the prepared samples were compared to the catalytic performance of commercial V-based system and aluminosilicate-based catalysts reported in the scientific literature. The natural aluminosilicates exhibited comparable activity in the satisfactory temperature range to the reference materials. Therefore, they have a big potential to be the precursors of NH<sub>3</sub>-SCR catalysts. In case of layered clays, despite the abundance in the environment and the low price, their application in NH<sub>3</sub>-SCR demands more effort than in case of the natural clinoptilolite. The preparation procedure of this zeolite-based catalyst is less complicated and cheaper. The material remains very active in NO conversion and selective to N<sub>2</sub> in spite of some structural changes caused by the initial modifications. Consequently, considering the most important features of the effective substitute for the commercial NH<sub>3</sub>-SCR catalyst, clinoptilolite-based system is the most promising among all of the discussed materials.

## Acknowledgments

The research was financed by AGH Grant 16.16.210.476.

## References

- ANDREOLI, S., DEORSOLA, F., A., GALLETTI, C., PIRONE, R. 2015. *Nanostructured MnO<sub>x</sub> catalysts for low-temperature NO<sub>x</sub> SCR*. Chem. Eng. J. 278, 174-182.
- BARBOOTI, M.M., IBRAHEEM, N.K., ANKOSH, A.H., 2011. *Removal of nitrogen dioxide and sulfur dioxide from air streams by absorption in urea solution*. J. Environ. Protect. 2, 175-185.
- BAZAN-WOZNIAK, A., NOWICKI, P., PIETRZAK, R., 2018. *Production of new activated bio-carbons by chemical activation of residue left after supercritical extraction of hops*. Environ. Res. 161, 456-463.
- CHEN, L., LI, J., GE, M., 2011. *The poisoning effect of alkali metals doping over nano V<sub>2</sub>O<sub>5</sub>-WO<sub>3</sub>/TiO<sub>2</sub> catalysts on selective catalytic reduction of NO<sub>x</sub> by NH<sub>3</sub>*. Chem. Eng. J., 170 (2-3), 531-537.
- CHMIELARZ, L., ZBROJA, M., KUŚTROWSKI, P., DUDEK, B., RAFALSKA-ŁASOCHA, A., DZIEMBAJ, R., 2004. *Pillared montmorillonites modified with silver. Temperature programmed desorption studies*. J. Therm. Anal. Calorim. 77, 115-123.
- CHMIELARZ, L., KOWALCZYK, A., MICHALIK, M., DUDEK, B., PIWOWARSKA, Z., MATUSIEWICZ, A., 2010. *Acid-activated vermiculites and phlogophites as catalysts for the DeNO<sub>x</sub> process*. Appl. Clay Sci. 49, 156-162.
- CHMIELARZ, L., KUŚTROWSKI, P., MICHALIK, M., DUDEK, B., PIWOWARSKA, Z., DZIEMBAJ, R., 2008. *Vermiculites intercalated with Al<sub>2</sub>O<sub>3</sub> and modified with transition metals as catalysts of DeNO<sub>x</sub> process*. Catal. Today 137, 242-246.
- CHMIELARZ, L., KUŚTROWSKI, P., PIWOWARSKA, Z., MICHALIK, M., DUDEK, B., DZIEMBAJ, R., 2009. *Natural micas intercalated with Al<sub>2</sub>O<sub>3</sub> and modified with transition metals as catalysts of the selective oxidation of ammonia to nitrogen*. Top. Catal. 52, 1017-1022.
- CHMIELARZ, L., KUŚTROWSKI, P., ZBROJA, M., RAFALSKA-ŁASOCHA, A., DUDEK, B., DZIEMBAJ, R., 2003. *SCR of NO by NH<sub>3</sub> on alumina or titania-pillared montmorillonite various modified with Cu or Co: Part I. General characterization and catalysts screening*. Appl. Catal. B. 45, 103-116.
- CHMIELARZ, L., PIWOWARSKA, Z., KUŚTROWSKI, P., WĘGRZYN, A., GIL, B., KOWALCZYK, A., DUDEK, B., DZIEMBAJ, R., MICHALIK, M., 2011. *Comparison study of titania pillared interlayered clays and porous clay heterostructures modified with copper and iron as catalysts of the DeNO<sub>x</sub> process*. Appl. Clay Sci. 53, 164-173.
- CHMIELARZ, L., WOJCIECHOWSKA, M., RUTKOWSKA, M., ADAMSKI, A., WĘGRZYN, A., KOWALCZYK, A., DUDEK, B., BOROŃ, P., MICHALIK, M., MATUSIEWICZ, A., 2012. *Acid-activated vermiculites as catalysts of the DeNO<sub>x</sub> process*. Catal. Today 191, 25-31.
- DAKDAREH, A.M., FALAMAKI, C., GHASEMIAN, N., 2018. *Hydrothermally grown nano-manganese oxide on clinoptilolite for low-temperature propane-selective catalytic reduction of NO<sub>x</sub>*. J. Nanopart. Res. 20, 309.
- DELIYANNI, E.A., KYZAS, G.Z., MATIS, K.A., 2017. *Various flotation techniques for metal ions removal*. J. Mol. Liq. 225, 260-264.
- DENG, S., ZHUANG, K., XU, B., DING, Y., YU, L., FAN, Y., 2016. *Promotional effect of iron oxide on the catalytic properties of Fe-MnO<sub>x</sub>/TiO<sub>2</sub> (anatase) catalysts for the SCR reaction at low temperatures*. Catal. Sci. Technol. 6, 1772-1778.
- DOULA, M.K., 2007. *Synthesis of a clinoptilolite-Fe system with Cu sorption capacity*. Chemosphere 67, 731-740.
- DOULA, M., IOANNOU, A., 2003. *The effect of electrolyte anion on Cu adsorption-desorption by Clinoptilolite*. Micropor. Mesopor. Mater. 58, 115-130.
- ENGLER, B.H., 1991. *Katalysatoren für den Umweltschutz*. Chem. Ing. Tech. 63 (4), 298.
- FENG, Q., WEN, S., BAI, X., CHANG, W., CUI, C., ZHAO, W., 2019. *Surface modification of smithsonite with ammonia to enhance the formation of sulfidization products and its response to flotation*. Miner. Eng. 137, 1-9.
- GAO, F., WASHINGTON, N.M., WANG, Y., KOLLÁR, M., SZANYI, J., PEDEN, C.H.F., 2015. *Effects of Si/Al ratio on Cu/SSZ-13 NH<sub>3</sub>-SCR catalysts: Implications for the active Cu species and the roles of Brønsted acidity*. J. Catal. 331, 25-38.
- GAO, F., ZHENG, Y., KUKKADAPU, R.K., WANG, Y., WALTER, E.D., SCHWENZER, B., SZANYI, J., PEDEN, C. H.F., 2016. *Iron loading effects in Fe/SSZ-13 NH<sub>3</sub>-SCR catalysts: Nature of the Fe ions and structure-function relationships*. ACS Catal. 6, 2939-2954.
- GELVES, J.-F., DORKIS, L., MÁRQUEZ, M.-A., ÁLVAREZ, A.-C., GONZÁLEZ, L.-M., VILLA, A.-L., 2019. *Activity of an iron Colombian natural zeolite as potential geo-catalyst for NH<sub>3</sub>-SCR of NO<sub>x</sub>*. Cat. Today, 320, 112-122.

- GRZYBEK, T., 2007. *Layered clays as SCR deNO<sub>x</sub> catalysts*. Catal. Today 119, 125-132.
- GUAN, B., ZHAN, R., LIN, H., HUANG, Z., 2014. *Review of state of the art technologies of selective catalytic reduction of NO<sub>x</sub> from diesel engine exhaust*. Appl. Therm. Eng. 66, 395-414.
- HAYATI-ASHTIANI, M., 2012. *Use of FTIR spectroscopy in the characterization of natural and treated nanostructured bentonites (montmorillonites)*. Particul. Sci. Technol. 30, 553-564.
- HIRANO, T., 1986. *Active phase in potassium-promoted iron oxide catalyst for dehydrogenation of ethylbenzene*. Appl. Catal. 26, 81-90.
- HUFF, W.D., 2016. *K-bentonites: A review*. American Mineral. 101, 43-70.
- HUO, X., WU, L., LIAO, L. XIA, Z., WANG, L., 2012. *The effect of interlayer cations on the expansion of vermiculite*. Powder Technol. 224, 241-246.
- JABŁOŃSKA, M., PALKOVITS, R., 2016. *Nitrogen oxide removal over hydrotalcite-derived mixed metal oxides*. Catal. Sci. Technol. 6, 49-72.
- KOWALCZYK, A., ŚWIĘŚ, A., GIL, B., RUTKOWSKA, M., PIWOWARSKA Z., BORCUC, A., MICHALIK, M., CHMIELARZ, L., 2018. *Effective catalysts for the low-temperature NH<sub>3</sub>-SCR process based on MCM-41 modified with copper by template ion-exchange (TIE) method*. Appl. Catal. B. 237, 927-937.
- KWON, D.W., PARK, K.H., HONG, S.C., 2016. *Enhancement of SCR activity and SO<sub>2</sub> resistance on VO<sub>x</sub>/TiO<sub>2</sub> catalyst by addition of molybdenum*. Chem. Eng. J. 284, 315-324.
- LIU, Z.G., OTTINGER, N.A., CREMEENS, C.M., 2015. *Vanadium and tungsten release from V-based selective catalytic reduction diesel aftertreatment*. Atmos. Environ. 104, 154-161.
- MADIA, G., KOEBEL, M., ELSENER, M., WOKAUN, A., 2002. *Side reactions in the selective catalytic reduction of NO<sub>x</sub> with various NO<sub>2</sub> fractions*. Ind. Eng. Chem. Res. 41, 4008-4015.
- MARTIN, N., VENNSTRØM, P.N.R., THØGERSEN, J.R., MOLINER, M., CORMA, A., 2017. *Iron-containing SSZ-39 (AEI) zeolite: An active and stable high-temperature NH<sub>3</sub>-SCR catalyst*. Chem. Cat. Chem. 9, 1754-1757.
- MOTAK, M., 2008. *Montmorillonites modified with polymer and promoted with copper as DeNO<sub>x</sub> catalysts*. Catal. Today 137, 247-252.
- NEZAMZADEH-EJHIEH, A., AMIRI, M., 2013. *CuO supported clinoptilolite towards solar photocatalytic degradation of p-aminophenol*. Powder Technol. 235, 279-288.
- NIU, C., SHI, X., LIU, F., LIU, K., XIE, L., YOU, Y., HE, H., 2016. *High hydrothermal stability of Cu-SAPO-34 catalysts for the NH<sub>3</sub>-SCR of NO<sub>x</sub>*. Chem. Eng. J., 294, 254-263.
- PAOLUCCI, C., DI IORIO, J.R., RIBEIRO, F.H., GOUNDER, R., SCHNEIDER, W.F., 2016. *Catalysis science of NO<sub>x</sub> selective catalytic reduction with ammonia over Cu-SSZ-13 and Cu-SAPO-34*. Adv. Catal. 59, 1-107.
- RAHKAMAA-TOLONEN, K., MAUNULA, T., LOMMA, M., HUUHTANEN, M., KEISKI, R.L., 2005. *The effect of NO<sub>2</sub> on the activity of fresh and aged zeolite catalysis in the NH<sub>3</sub>-SCR reaction*. Catal. Today 100, 217-222.
- REY-PEREZ-CABALLERO, F.J., PONCELET, G., 2000. *Al-pillared vermiculites: Microporous 18A preparation and characterization*. Micropor. Mesopor. Mater. 37, 313-327.
- RUTKOWSKA, M., PACIA, I., BASAĞ, S., KOWALCZYK, A., PIWOWARSKA, Z., DUDA, M., TARACH, K.A., GÓRA-MAREK, K., MICHALIK, M., DIAZ, U., CHMIELARZ, L., 2017. *Catalytic performance of commercial Cu-ZSM-5 zeolite modified by desilication in NH<sub>3</sub>-SCR and NH<sub>3</sub>-SCO process*. Micropor. Mesopor. Mater. 246, 193-206.
- RYU, T., KANG, Y., NAM, I.-S., HONG, S.-B., 2019. *Iron-exchanged high-silica LTA zeolites as hydrothermally stable NH<sub>3</sub>-SCR catalysts*. React. Chem. Eng. 4, 1050-1058.
- SAAD, M., BIAŁAS, A., CZOSNEK, C., MOTAK, M., 2019. *Tlenkowe katalizatory cerowo-miedziowe naniesione na węgiel do niskotemperaturowego usuwania NO<sub>x</sub> ze stacjonarnych źródeł emisji*. Przem. Chem. 98(4), 546-550.
- SAMOJEDEN, B., GRZYBEK, T., 2016. *The influence of the promotion of N-modified activated carbon with iron on NO removal by NH<sub>3</sub>-SCR (Selective catalytic reduction)*. Energy 116, 1484-1491.
- SAMOJEDEN, B., DRUŻKOWSKA, J., DURACZYŃSKA, D., PODDĘBNIĄK, M., MOTAK, M., 2019a. *Use of iron and copper-promoted cenospheres as catalysts in the selective catalytic reduction of nitrogen(II) oxide with ammonia*. Przem. Chem., 98(4), 541-545.
- SAMOJEDEN, B., GRZYBEK, T., SZYMASZEK, A., LIGĘZA, O., KOWALCZYK, W., MOTAK, M., 2019b. *The application of modified cenospheres in DeNO<sub>x</sub> process*. E3S Web of Conferences 108 (02019), 1-8
- SANTOS, S.S.G., SILVA, H.R.M., DE SOUZA, A.G., ALVES, A.P.M., DA SILVA FILHO, E.C., FONESECA, M.G., 2015. *Acid-leached mixed vermiculites obtained by treatment with nitric acid*. Appl. Clay Sci. 104, 286-294.
- SHEN, B., MA, H., HE, C., ZHANG, X., 2014. *Low temperature NH<sub>3</sub>-SCR over Zr and Ce pillared clay based catalysts*. Fuel Process. Technol. 119, 121-129.

- ŚLIWIŃSKA-DĄBROWSKA, R., SCHMIDT, R., SIKORA, A., 2011. Właściwości fizykochemiczne zeolitu modyfikowanego jonami żelaza. *Inżynier. Ekol.* 24, 195-204.
- STAWIŃSKI, W., WĘGRZYN, A., DAŃKO, T., FREITAS, O., FIGUEIREDO, S., CHMIELARZ, L., 2017. Acid-base treated vermiculite as high performance adsorbent: Insights into the mechanism of cationic dyes adsorption, regeneration, recyclability and stability studies. *Chemosphere*, 173, 107-115.
- STRIVASTAVA, R.K., NEUFFER, W., GRANO, D., KHAN, S., STAUDT, J.E., JOZEWICZ, W., 2005. Controlling NO<sub>x</sub> emission from industrial sources. *Environ. Prog.* 24(2), 181-197.
- WANG, A., WANG, Y., WALTER, E.D., WASHINGTON, N.M., GUO, Y., LU, G., PEDEN, C.H.F., GAO, F., 2019. NH<sub>3</sub>-SCR on Cu, Fe and Cu + Fe exchanged beta and SSZ-13 catalysts: Hydrothermal aging and propylene poisoning effects. *Catal. Today* 320, 91-99.
- WANG, L., WEI, L., SCHMIEG, S.J., WENG, D., 2015. Role of Brønsted acidity in NH<sub>3</sub> selective catalytic reduction reaction on Cu/SAPO-34 catalysts. *J. Catal.* 324, 98-106.
- WECKHUYSEN, B.M., YU, J., 2015. Recent advances in zeolite chemistry and catalysis. *Chem. Soc. Rev.* 44, 7022-7024.
- WIERZBICKI, D., DĘBEK, R., SZCZUROWSKI, J., BASAĞ, S., WŁODARCZYK, W., MOTAK, M., BARAN, R., 2015. Copper, cobalt and manganese: Modified hydrotalcite materials as catalysts for the selective catalytic reduction of NO with ammonia. The influence of manganese concentration. *C. R. Chim.* 18, 1074-1083.
- WU, W., CHENG, L.C., SHEN, L.S., ZHANG, K., MENG, H., GUO, K., CHEN, J.F., 2009. Effects of silica sources on the properties of magnetic hollow silica. *Colloid. Surf. A*, 334, 131-136.
- YANG, S., FU, Y., LIAO, Y., XIONG, S., QU, Z., YAN, N., LI, J., 2014. Competition of selective catalytic reduction and non selective catalytic reduction over MnO<sub>x</sub>/TiO<sub>2</sub> for NO removal: the relationship between gaseous NO concentration and N<sub>2</sub>O selectivity. *Catal. Sci. Technol.* 4(1), 224-232.
- YIN, W., HAN, Y., XIE, F., 2010. Two-step flotation recovery of iron concentrate from Donganshan carbonaceous iron ore. *J. Cent. South Univ. Technol.* 17, 750-754.
- YUAN, M., DENG, W., DONG, S., LI, Q., ZHAO, B., SU, Y., 2018. Montmorillonite based porous clay heterostructures modified with Fe as catalysts for selective catalytic reduction of NO with propylene. *Chem. Eng. J.* 353, 839-848.
- ZHANG, S.-H., CAI, L.-L., MI, X.-H., JIANG, J.-L., LI, W., 2008. NO<sub>x</sub> Removal from simulated flue gas by chemical absorption - biological reduction integrated approach in biofilter. *Environ. Sci. Technol.* 42(10), 3814-3820.
- ZHAO, W., LIU, D., FENG, Q., WEN, S., CHANG, W., 2019. DFT insights into the electronic properties and adsorption mechanism of HS<sup>-</sup> on smithsonite (101) surface. *Miner. Eng.* 141, 105846.
- ZHIRONG, L., AZHAR UDDIN, M.D., ZHANXUE, S., 2011. FT-IR and XRD analysis of natural Na-bentonite and Cu(II)-loaded Na-bentonite. *Spectrochim. Acta A*, 79, 1013-1016.
- ZIEMIAŃSKI, P., KAŁAHURSKA, K., SAMOJEDEN, B., 2015. Selective catalytic reduction of NO with NH<sub>3</sub> on mixed alumina-iron (III) oxide pillared montmorillonite "Cheto" Arizona, modified with hexamminecobalt (III) chloride. *Adsorpt. Sci. Technol.* 35, 825-833.